15th IAPR International Conference on Machine Vision Applications (MVA)
Nagoya University, Nagoya, Japan, May 8-12, 2017.

Real-time Image Improvement System for Visual Testing of Nuclear Reactors

Naoki Hosoya
Hitachi, Ltd.
Totsuka-ku, Yokohama-shi, Kanagawa, Japan
naoki.hosoya.bj@hitachi.com

Atsushi Miyamoto
Hitachi, Ltd.
Totsuka-ku, Yokohama-shi, Kanagawa, Japan
atsushi.miyamoto.ts@hitachi.com

Junichirou Naganuma
Hitachi-GE Nuclear Energy, Ltd.
Saiwai-cho, Hitachi-shi, Ibaraki, Japan
junichirou.naganuma.vt@hitachi.com

Abstract

In nuclear power plants, visual testing (VT) based on video images taken from an underwater camera is carried out. However, it is a problem in that a lot of noise is superimposed on VT images due to radiation exposure. We propose a technique for improving the quality of those images by image processing that includes radiation noise reduction and signal enhancement. Real-time video processing was realized by applying the proposed technique with a parallel processing unit. Improving the clarity of VT images will lead to a reduced burden placed on inspectors.

1. Introduction

In nuclear power plants, in-vessel testing is periodically conducted to check for soundness or for preventive maintenance [1]. One inspection procedure that is carried out is visual testing (VT), which is based on video images taken from an underwater camera [2]. If defect candidates are found in VT, detailed inspections, such as ultrasonic testing and eddy current testing [3][4], are conducted. Therefore, VT images with high clarity are required for reliable inspection. However, it is a problem in that a lot of noise is superimposed on VT images due to radiation exposure. To overcome this, we propose a technique for improving the quality of VT images by image processing that includes radiation noise reduction and signal enhancement.

2. Real-time video image improvement system

Figure 1 illustrates the proposed VT image improvement system. Inspectors conduct VT on the basis of the color video images of around 400,000 pixels that are taken from an underwater camera. There often exist several hindrances in VT images, such as radiation noise and low contrast. Since the inner vessel is a radiation field, a lot of radiation noise is superimposed on images. In addition, the illumination used for imaging may not be enough, especially in such a narrow space. This motivated us to improve the clarity of VT images by image processing to reduce the burden placed on inspectors. Our proposed system includes three functions:

・radiation noise reduction,
・signal enhancement, and
・real-time processing (30 frames/s).

3. Algorithms

3.1. Noise reduction

Noise reduction techniques can be broadly classified into two groups: the spatial filter technique and the time filter technique [5]. While radiation noise components are independent among sequential image frames, signal components have a strong correlation among the frames. We thus decided to use a time filter**.**

The noise on current frame f_n is reduced by addition average among all f_n and the aligned past frames $\{f'_{n-k}\}$ (k = 1~K, K: number of past frames). As shown in Fig. 2(b), the current frame f_n is divided into multiple rectangular templates $\{T_i\}$ [$i \in \Omega_l$, $\Omega_l=(1,2,...,N_l)$, N_l: number of the templates] called "local templates." A displacement vector ($\Delta x_{i,k}$, $\Delta y_{i,k}$) is obtained by matching f_n with f_{n-k} for ith template. The aligned past frames are given as $f'_{n-k}[x,y] = f_{n-k}[x-\Delta x_{i,k}, y-\Delta y_{i,k}]$. A noise reduction image, g_n, can be calculated as follows.

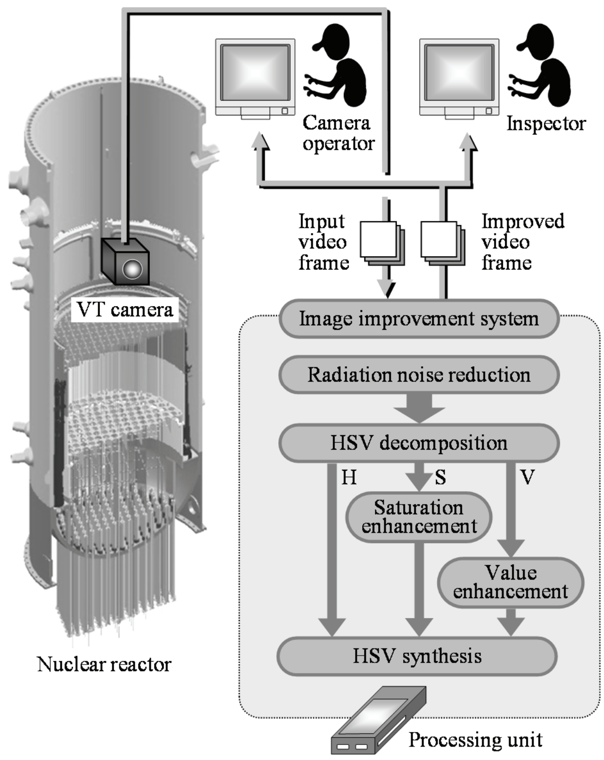

Fig.1 Video image improvement system

© 2017 MVA Organization

$$g_n[x,y] = M\left(\frac{1}{K} f_n[x,y] + \sum_{k=1}^{K} W_k\left(\frac{\mathrm{SAD}_k[x,y]}{m[x,y]^2}\right) f'_{n-k}[x,y]\right), \quad (1)$$

where M is the reciprocal number of the sum of the frame weight, $\mathrm{SAD}_k[x,y]$ is the sum of the absolute difference between f_n and f'_{n-k} in the region near [x,y], m is the standard deviation among the high-pass filtered frames, and $W(a)$ is the monotone decreasing function for a (maximum: $1/K$, minimum: 0).

The weight W should be set small in the region where the difference in the signal components between frames is large. SAD is changed not only by the difference but the quantity of noise. Therefore, W is calculated on the basis of both SAD_k and m.

3.2. Signal enhancement

Stress corrosion cracking (SCC) is one of the most representative defects to be inspected. SCC is often observed as a slightly vivid crack because of corrosion. After noise reduction, we convert an RGB color image $g_n = (r, g, b)$ into an HSV color image (h, s, v), which consists of three components: hue, saturation, and value [6]. Since the saturation in the SCC region is assumed to be high, the high-frequency component of s is strongly emphasized. Similarly, since the value in the region of the vessel structure is assumed to be high, the high-frequency component of v is emphasized. To avoid the amplification of residual noise on g_n, a low-path filter is applied to g_n before the saturation and signal enhancement. The output image $g_{\mathrm{sig},n}$ is

$$g_{\mathrm{sig},n} = \mathrm{RGB}(h, E(s), E(v)), \quad (2a)$$

$$E(a) = a - (L(a) - B(L(a))) + G(L(a) - B(L(a))). \quad (2b)$$

Here $L()$, $B()$, $G()$ are the low-pass filter, bilateral filter [7], and gamma correction. The term $L(b)-B(L(b))$ in the equation (2b) is the high frequency component of the residual noise reduction image. The high frequency component is selectively emphasized by gamma correction.

3.3. Acceleration of correspondence search between frames

Generally, the computational cost of correlated calculation is high. To speed up the template matching among the frames mentioned in section 3.1, global and local matching are adopted as shown in Fig. 2.

A few characteristic templates $\{T_i\}$ ($i \in \Omega_g \subseteq \Omega_l$), called "global templates," are selected from a local template group. The characteristic degrees are evaluated by the number of edge segments extracted by a differential filter. Figure 2(a) shows displacement vectors between the current frame and the past frame at the positions of the global templates. The displacement vectors of the local templates can be calculated quickly by using the hill-climbing method [8] with adequate initial values, which are estimated by linear interpolation of the displacement vectors of global templates.

Template matching may sometimes fail due to image noise in a strong radiation field. To improve the reliability, a robust algorithm for removing outlying matching results is included. In global matching, unreliable vectors satisfying the following condition are removed as shown in Fig. 3(a).

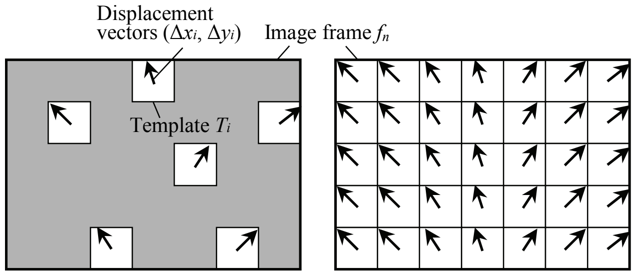

(a) Global matching (b) Local matching

Fig.2 Template matching between frames

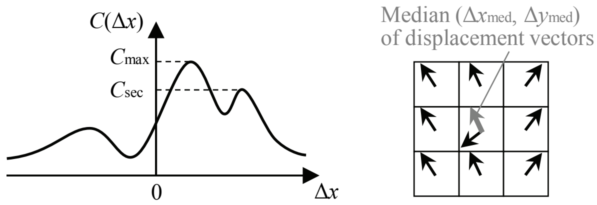

(a) Global matching (b) Local matching

Fig.3 Excluding matching results with low reliability

$$C_{\max} - C_{\sec} < p_1, \quad (3)$$

where, $C_{\max}$ is the maximum correlation value, and $C_{\sec}$ is the second one, which satisfies the convex condition, that is, $C_{\sec}$ is higher than the correlation values at its neighboring pixels. The variable p_1 is a parameter. In local matching, dense vectors can be provided. As illustrated in Fig. 3(b), outlying vectors, not neighboring vectors, are removed and interpolated according to the following equation.

$$(\Delta x, \Delta y) = \begin{cases} (\Delta x, \Delta y) & \text{if } \sqrt{(\Delta x - \Delta x_{\mathrm{med}})^2 + (\Delta y - \Delta y_{\mathrm{med}})^2} < p_2, \\ (\Delta x_{\mathrm{med}}, \Delta y_{\mathrm{med}}) & \text{otherwise} \end{cases} \quad (4)$$

where (Δx_{med}, Δy_{med}) is median of the displacement vector in the neighboring eight templates, and p_2 a is parameter.

4. Experimental results

We implemented the proposed algorithm into a parallel processor, that is, a graphics processing unit (GPU), and improved the real-time display of video images. Figure 4 is a screen shot showing the result. Input and output images are displayed on the left and right side of the figure.

4.1. Image evaluation

The VT images were simulated to discuss the effectiveness of the proposed technique in changing the quantity of noise. The color filters in the CCD camera were arranged in a Bayer pattern, and the RGB values were provided by adaptive color plane interpolation (ACPI) [9]. From the CCD element value e_0 without radiation noise, the value e with noise is calculated by the following equation.

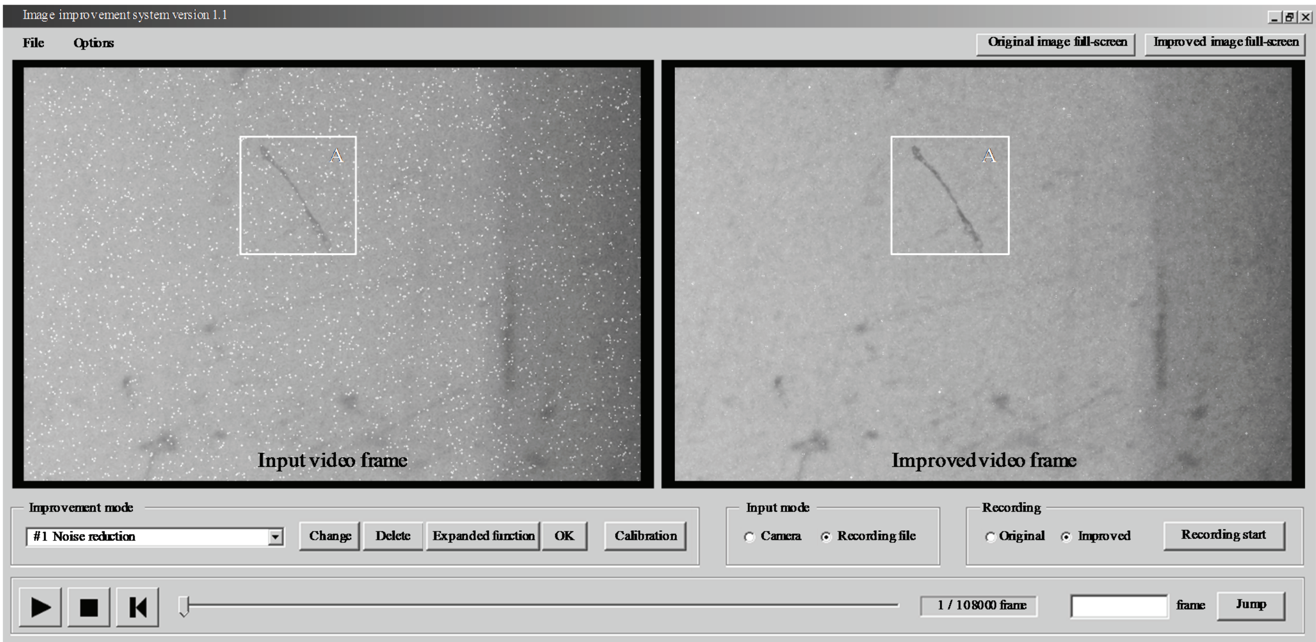

Fig.4 Screen shot showing result

$$e[i,j] = \min\left(e_0[i,j] + \sum_{\delta i, \delta j}\left(n_r[i+\delta i, j+\delta j]G(\sigma_n)[\delta i, \delta j]\right), 255\right),$$

$$n_r[i,j] = \begin{cases} 255 & if\ |r| > R \\ 0 & otherwise \end{cases},$$

$$G(\sigma_n)[i,j] = \exp\left(-\frac{i^2 + j^2}{2\sigma_n^{\ 2}}\right), \qquad (5)$$

where r is normally distributed random numbers with a mean of 0.0 and variance of 1.0, and R is a parameter. In the equation (5), it is assumed that one radiation pulse collides with one pixel.

The RGB values are calculated from e by ACPI. As parameter R is set to be small, a lot of noise is imposed on the simulated image.

Figure 5 is expanded images of region A in Fig. 4, and a crack can be observed as a black line. Figures 5 (a), (b), and (c) are the input image, an image showing the noise reduction proposed in section 3.1, and an image of the signal enhancement proposed in section 3.2. The proposed technique could effectively enhance the crack without noise amplification, improving its visibility.

Figures 6 (a) and (b) are saturation and value components of an HSV image after noise reduction. Since the saturation of the crack seems to be high, the crack can be selectively enhanced in the improved image.

The quality of the improved image is quantitatively evaluated by using the contrast-to-noise ratio (CNR) [10] [11]. Figure 7 (a) shows the CNR improvement ratio between the input image and improved image for a variation of noise amounts (horizontal axis), which are adjusted by changing R in equation (6). Although the effects differ according to the noise amount, the noise reduction proposed in section 3.1 and signal enhancement proposed in section 3.2 improved CNR to 1.3 - 3.0 times and 2.0 - 4.0 times. The CNR improvement ratio in Figs. 7(a) is separated into the contrast improvement ratio and noise reduction ratio in Figs. 7(b) and (c), respectively. As we can see from the change in the noise reduction ratio before and after signal enhancement, enough noise was removed and was not amplified. Therefore, the effect of contrast improvement leads to improving the CNR directly.

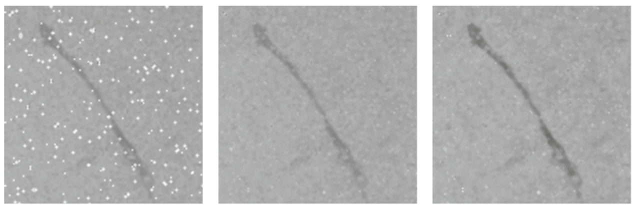

(a) Input image (b) Noise reduction (c) Signal enhancement

Fig.5 Enlarged images of region A in Fig.4

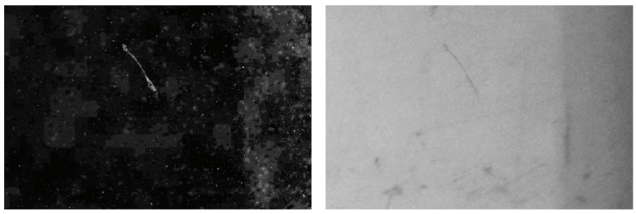

(a) Saturation (b) Value

Fig.6 HSV component images

4.2. Processing time

Figure 8 shows the processing time of image improvement. For real-time display, the processing time per one frame needs to be less than 33ms. The acceleration algorithm proposed in section 3.3 reduced the processing cost of correspondence search, which accounts for most of the whole processing time. The total processing time in the CPU was reduced from 31 s to 4 s (left and middle bars in Fig. 8). Furthermore, the parallelization done by using a GPU shortened the processing time to 23 ms (right bar in Fig. 8), resulting in real-time display.

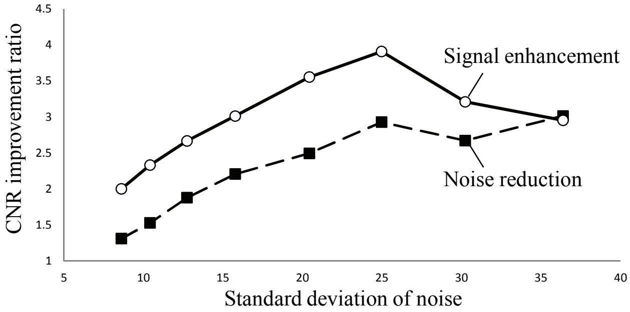

(a) CNR improvement ratio

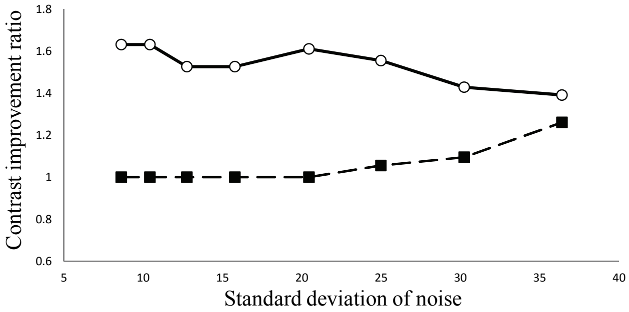

(b) Contrast improvement ratio

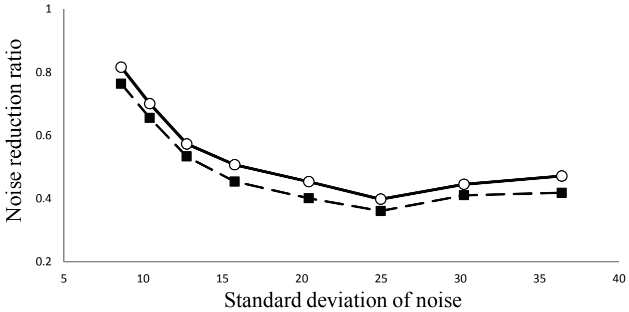

(c) Noise reduction ratio

Fig.7 CNR improvement ratio between input image and improved image

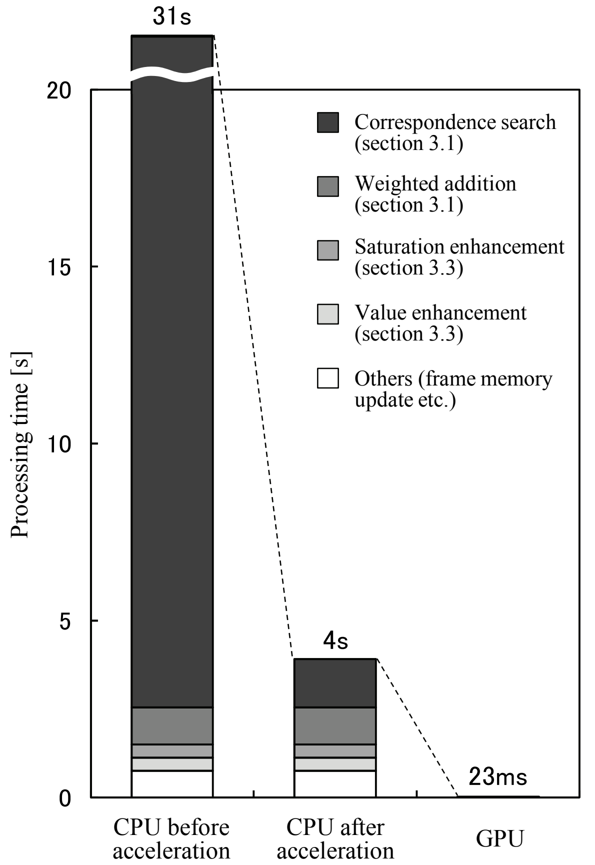

Fig.8 Processing time

5. Conclusion and future work

In this study, we developed a real-time image improvement system for VT in nuclear reactors. We proposed robust and fast image processing to improve the quality of VT images, which can suffer from noise due to strong radiation effects. Experimental results demonstrated the significance of the proposed method. For future work, it is necessary to verify the effectiveness of our system in real reactors continuously. The practicality of using the technique to check soundness or for preventive maintenance may be promoted.

References

[1] T. Ikegami, T. Shimura, and M. Koike: “Plant Life Management and Maintenance Technologies for Nuclear Power Plants,” Hitachi Review, vol.50, no.3, pp.84-88, 2001.

[2] M. Odakura, M. Kometani, M. Koike, M. Tooma, and Y. Nagashima: “Advanced Inspection Technologies for Nuclear Power Plants,” Hitachi Review, vol.58, no.2, pp.82-87, 2009.

[3] I. Komura, T. Hirasawa, S. Nagai, J. Takabayashi, and K. Naruse: “Crack Detection and Sizing Technique by Ul trasonic and Electromagnetic Methods,” Nuclear Engineering and Design, vol.206, no.2-3, pp.351-362, 2001.

[4] S. Kitazawa, M. Odakura, K. Otani, and Y. Adachi: “Advanced Inspection Technologies for Energy Infrastructure,” Hitachi Review, vol.59, no.3, pp.111-115, 2010.

[5] A. Rosenfeld and A. C. Kak: Digital Picture Processing, Academic Press, 1976.

[6] A. R. Smith: “Color Gamut Transform Pairs,” Proc. of Conf. on ACMSIGGRAPH, vol.78, pp.12-18, 1978.

[7] C. Tomasi and R. Manduchi: “Bilateral Filtering for Gray and Color Images,” Proc. of IEEE Int. Conf. on Computer Vision, pp. 836-846, 1998.

[8] B. D. Lucas and T. Kanade: “An Iterative Image Rregistration Technique with an Application to Stereo Vision,” Proc. of Imaging Understanding Workshop, pp.121-130, 1981.

[9] R. Ramanath, W. E. Snyder, and G. L. Bilbro: “Demosaicking Methods for Bayer Color Arrays,” Journal of Electronic Imageing, vol.11, no.3, pp.306-315, 2002.

[10] D. Shao and D. C. Liu: “Local Histogram Matching Based Bilateral Filter to Ultrasound Speckle Reduction,” Proc. 5th IEEE Int. Conf. Bioinformatics and Biomedical Engineering, pp.1-4, 2011.

[11] A. E. Petropoulos, G. F. Vlachopoulos, S. G. Skiadopoulos, A. N. Karahaliou and L. I. Costaridou: “Improving Image Quality in Dual Energy CT by Edge-Enhancing Diffusion Denoising,” Proc. 13th IEEE Int. Conf. Bioinformatics and Bioengineering, pp.1-4, 2013.